Monitoring cellular metabolism of 3T3 upon wild type *E. coli* infection by mapping NADH with FLIM

(Invited Paper)

Tatyana Buryakina[1], Pin-Tzu Su[2], Vladimir Gukassyan[1], Wan-Jr Syu[2], and Fu-Jen Kao[1,3*]

[1] *Institute of Biophotonics and* [2] *Institute of Microbiology and Immunology, National Yang-Ming University, 155, Linong St., Sec. 2, Taipei 112, China*

[3] *Department of Photonics, National Sun Yat-Sen University, 70 Lien Hai Road, Kaohsiung 804, China*

[*] *E-mail: fjkao@ym.edu.tw*

Received June 13, 2010

Fluorescence lifetime imaging microscopy (FLIM) has gained popularity as a sensitive technique to monitor the functional/conformational states of reduced nicotinamide adenine dinucleotide (NADH), one of the main compounds of oxidative phosphorylation. In this letter, we apply the technique to characterize the metabolic changes in mouse embryonic fibroblast 3T3 cells upon bacterial infection. A gradual shortening of the decaying time constants in both the short and the long lifetime components of NADH's autofluorescence is detected. The ratio of the short and the long lifetime components' relative contributions, however, shows a rapid increase, indicating the rise of cellular metabolic activity over the course of infection.

OCIS codes: 000.1430, 000.4920, 110.1080, 180.2520, 180.4315, 300.2530.
doi: 10.3788/COL20100810.0931.

Reduced nicotinamide adenine dinucleotide (NADH) serves as a co-enzyme and a principal electron donor within the cell for both oxidative phosphorylation (aerobic respiration) and glycolysis (anaerobic respiration). This molecule exists in two functional forms: free and bound, whereas the latter is associated mostly with the dehydrogenases of so called Complex I-one of 4 mitochondrial membrane protein complexes, which mediate electron transfer from NADH to O_2 and use this flow to pump the hydrogen protons to the mitochondrial intermembrane space from the matrix[1]. This gradient of protons and electrical potential, termed proton-motive force, is utilized to synthesize new adenosine triphosphate (ATP) molecules at ATP-synthase via adenosine diphosphate (ADP) phosphorylation[2]. Thus NADH bound forms can be associated with the energy generation in the form of ATP, and the relative quantities of free and bound species of this coenzyme can give an insight on the metabolic state of a cell.

Bacterial infections and their influence on cellular physiology are of critical interest to researchers in broad areas, such as microbiology, medicine, drug design, etc. It has been shown that O157:H7 serotype of *Escherichia coli* (*E. coli*), an important human pathogen, closely adheres to the gut epithelium and activates an effacement of the brush border microvilli, a phenomenon known as attaching and effacing[3]. Adhesion of enteropathogenic *E. coli* to epithelial cells also triggers actin-rich pedestal formation beneath the bacteria[4]. By some uncharted mechanisms, *E. coli* can induce apoptosis in a number of epithelial cell lines[5]. All these studies suggest the importance of characterizing the cellular metabolism as a result of bacterial infection.

A number of different techniques have been applied for these studies, of which fluorescence spectra microscopy has gained wide acceptance because of the high sensitivity, the high spatial resolution, and the ability to investigate the molecular processes of living pathogens in their host cells[6]. In particular, fluorescence lifetime imaging microscopy (FLIM), Förster resonance energy transfer (FRET), fluorescence recovery after photobleaching (FRAP), and fluorescence correlation spectroscopy (FCS) are shown to be powerful techniques to reveal the various stages and pathways of bacterial infection[7].

Based on the measurement of the average time fluorescent molecules spent on the excited states upon light absorption, FLIM can detect molecular interactions and changes in the immediate molecular nano-environments, as the corresponding pathways of energy relaxation are modified.

Free NADH in aqueous solution at room temperature has a mean fluorescence lifetime of ∼0.4 ns; whereas protein bound NADH has significantly higher values of ∼2.5 ns. The shortening of the lifetime is accounted by self-quenching of nicotinamide by the adenine moiety in folded free forms and is prevented upon spreading on the substrate[8,9]. At this, bound forms are usually associated with the NADH molecules bound to mitochondrial membrane protein complex thus participating in the ATP generation.

Understanding these dynamics may elucidate the bioenergetics of cells in culture and will allow proper characterization of the range of free/bound changes in normal state, which will provide a standard in studying cellular pathologies. The applications of FLIM for metabolism mapping in cells have been demonstrated earlier[10,11]. Here we apply FLIM to investigate cellular metabolism upon bacterial infection. For this purpose, a culture of 3T3 cells has been imaged during 4 h after incubation with the wild-type *E. coli*. The characteristic changes in metabolism are reflected in the ratio of relative contributions from free and bound species (a_1/a_2) as well as in the free and bound species' lifetimes (t_1 and t_2).

Mouse embryonic epithelial fibroblast cells, NIH 3T3, were seeded at 3×10^5 concentration on 24-mm round

glass cover slips (Deckglaser) coated with poly-L-lysine (Sigma Inc.) and incubated overnight. The cells were then washed with phosphate-buffered saline (PBS) and replenished with phenol red-free DMEM (Gibco BRL). The infection of wild-type *E. coli* O157:H7 was introduced to the cells at a dilution of 1:50 with further incubation for 1 h. After infection the cover slips were washed with PBS and then overlaid with phenol red-free DMEM.

For the NADH FLIM observation, infected and control cells were excited (under two-photon mode) by a mode-locked Ti:sapphire Mira F-900 laser (Coherent Inc.) operating at 740 nm. The beam was coupled to the FV300 scanning unit (Olympus Corp.)[12] and focused on the sample with a 60×, numerical aperture NA=1.45 oil-immersion objective (Olympus Corp.). An average laser power within 4 mW above the objective was used throughout the imaging sessions to prevent photodamage of the sample. The measurements were conducted on a modified inverted Olympus microscope (IX 71) completed with incubator (Oko Lab S.r.l) to maintain the viable physiological and physicochemical conditions (37 °C, 5% CO_2). The autofluorescence from NADH was detected in a non-descanned manner by a thermo-electrically cooled GaAsP photomultiplier tube (H7422-P40, Hamamatsu Photonics K.K.). A band-pass filter (447±30 nm, Semrock Inc.) was used to match the spectral characteristics of NADH autofluorescence.

Signals synchronization and storage of time-resolved data matrix were conducted by the SPC-830 time-correlated single photon counting (TCSPC) board (Becker&Hickl GmbH)[13]. All the images were taken at a resolution of 256×256 pixels with the acquisition time varying in the range of 500–700 s. No significant change of the photon count rate has been detected during the measurements. Data analysis and image reconstruction were done with the SPCImage v2.8 software package (Becker&Hickl GmbH) as described earlier[14].

In each imaging session, infected cells were observed continuously for 4 h until the cells ceased to survive, which was determined by the morphology of the cells. Measurements on intact 3T3 cell culture were also carried out as a controlled comparison. The corresponding FLIM images, exhibited as a_1/a_2 ratios, are shown in Fig. 1.

At the initial phase of infection, a relatively low a_1/a_2 ratio was observed when compared with the control measurement. The a_1/a_2 ratio increased gradually, as illustrated in Fig. 1(a), with the color-coded change from green to blue (colorful online). The corresponding peak values of the histograms are summarized in Table 1 and Fig. 1(b), with the results averaged for each hour after the infection (minimum 5 measurements per hour). The ratio of relative contributions

Table 1. Hourly Averaged Summaries from At Least Five Measurements of the Peak Values from the a_1/a_2 Distribution Histograms

	Infected				Control
	1 h	2 h	3 h	4 h	
a_1/a_2	3.124	3.448	4.006	4.33	4.285
	±0.28	±0.21	±0.16	± 0.15	± 0.23

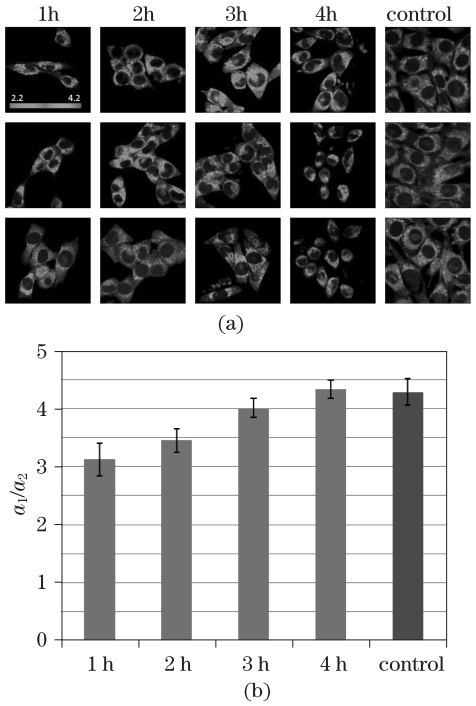

Fig. 1. Time-lapse dynamics of the a_1/a_2 ratio of the infected cells. (a) Representative FLIM images of infected and control 3T3 cells. The images are color-coded with the a_1/a_2 ratio. (b) Column bar chart for the peak values of the a_1/a_2 histograms, averaged for each hour after the infection and for one hour for the control. The error bar signifies standard deviation of the ratio for entire measurements.

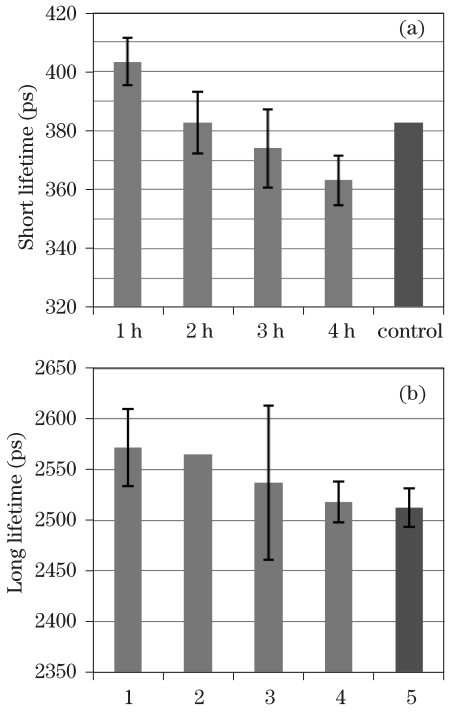

Fig. 2. Time-lapse distribution of (a) free and (b) protein bound NADH after infection. The error bar signifies standard deviation of the short lifetime for the entire measurements. The column bar charts are peak values of the free and bound NADH lifetimes histograms, averaged for each hour after the infection and for one hour for the control.

of free and protein bound NADH exhibits a gradual increase from 3.124±0.28 for the first hour to 4.33±0.15 at the fourth hour with the control value of a_1/a_2 equal to 4.285±0.22.

A gradual decrease in both short and long lifetime components (τ_1 and τ_2), originating from free and bound NADH species was detected, as illustrated in Fig. 2. A well distinguished decrease is shown for the short lifetime component (τ_1) and a less pronounced, however distinguishable, decrease is also shown for the long lifetime component (τ_2) of NADH.

With the use of FLIM on NADH autofluorescence, we have monitored the evolution of the relative contributions from the free and the bound forms of NADH, a feasible metabolic indicator for cells, caused by the bacterial infection. The shortening in the lifetimes may have also originated from the alternation of the cellular nano-environments that are related to the cellular physiology in response to the pathogen effects. Though further studies are required for in-depth assessment and understanding of the phenomena observed, resolving NADH autofluorescence with FLIM has already brought about interesting information on the cellular metabolic response to bacterial infection.

We appreciate greatly the generous support from the National Science Council (NSC 97-3112-B-010-006, NSC 96-2112-M-010-001, and NSC98-2112-M-010-001-MY3) and the Ministry of Education (Aim for Top University Project).

References

1. H. Lodish, A. Berk, C. A. Kaiser, M. Krieger, M. P. Scott, A. Bretscher, H. Ploegh, and P. Matsudaira, *Molecular Cell Biology* (W. H. Freeman and Co., New York, 2003).
2. B. Alberts, A. Johnson, J. Lewis, M. Raff, K. Roberts, P. Walter, *Molecular Biology of the Cell* (Garland Science, New York, 2007).
3. A. Mousnier, A. Whale, S. Schuller, J. Leong, A. Phillips, and G. Frankel, Infect. Immun. **76,** 4669 (2008).
4. K. Smith, D. Humphreys, P. Hume, and V. Koronakis, Cell Host and Microbe **7,** 13 (2010).
5. M. Abul-Milh, Y. Wu, B. Lau, C. Lingwood, and D. Forster, Infect. Immun. **69,** 7356 (2001).
6. J. Enninga, P. Sansonetti, and R. Tournebize, Trends Microbiol. **15,** 483 (2007).
7. F. Frischknecht, O. Renaud, and S. L. Shorte, Curr. Opin. Microbiol. **9,** 297 (2006).
8. B. Kierdaszuk, H. Malak, I. Gryczynski, P. Callis, and J. Lakowicz, Biophys. Chem. **62,** (1996).
9. A. Visser and A. Hoek, Photochem. Photobiol. **33,** 35 (1981).
10. H. W. Wang, V. Ghukasyan, C. T. Chen, Y. H. Wei, H. W. Guo, J. S. Yu, and F. J. Kao, J. Biomed. Opt. **13,** 054011 (2008).
11. V. Ghukasyan and F. J. Kao, J. Phys. Chem. C **113,** 11532 (2009).
12. V. Ghukasyan, Y. Y. Hsu, S. H. Kung, and F. J. Kao, J. Biomed. Opt. **12,** 024016 (2007).
13. W. Becker, *Advanced Time-Correlated Single Photon Counting Techniques* (Springer, Berlin, 2005).
14. V. Ghukasyan, C. C. Hsu, C. R. Liu, F. J. Kao, and T. H. Cheng, J. Biomed. Opt. **15,** 016008 (2010).